Development of the Proximal-Anterior Skeletal Elements in the Mouse Hindlimb Is Regulated by a Transcriptional and Signaling Network Controlled by *Sall4*

Katherine Q. Chen,* Naoyuki Tahara,*,†,‡ Aaron Anderson,*,[1] Hiroko Kawakami,*,†,‡ Sho Kawakami,* Ryuichi Nishinakamura,[§] Pier Paolo Pandolfi, and Yasuhiko Kawakami*,†,‡,[2]**

*Department of Genetics, Cell Biology and Development, †Stem Cell Institute, Minneapolis, Minnesota 55455, and ‡Developmental Biology Center, University of Minnesota, Minneapolis, Minnesota 55455, §Department of Kidney Development, Institute of Molecular Embryology and Genetics, Kumamoto University, Kumamoto, Japan 860-0811, and **Cancer Research Institute, Beth Israel Deaconess Cancer Center, Department of Medicine and Pathology, Beth Israel Deaconess Medical Center, Harvard Medical School, Boston, Massachusetts 02215

ORCID IDs: 0000-0003-1797-5229 (A.A.); 0000-0002-5413-7171 (S.K.); 0000-0002-0043-9705 (Y.K.)

ABSTRACT The vertebrate limb serves as an experimental paradigm to study mechanisms that regulate development of the stereotypical skeletal elements. In this study, we simultaneously inactivated *Sall4* using *Hoxb6Cre* and *Plzf* in mouse embryos, and found that their combined function regulates development of the proximal-anterior skeletal elements in hindlimbs. The *Sall4*; *Plzf* double knockout exhibits severe defects in the femur, tibia, and anterior digits, distinct defects compared to other allelic series of *Sall4*; *Plzf*. We found that *Sall4* regulates *Plzf* expression prior to hindlimb outgrowth. Further expression analysis indicated that *Hox10* genes and GLI3 are severely downregulated in the *Sall4*; *Plzf* double knockout hindlimb bud. In contrast, PLZF expression is reduced but detectable in *Sall4*; *Gli3* double knockout limb buds, and SALL4 is expressed in the *Plzf*; *Gli3* double knockout limb buds. These results indicate that *Plzf*, *Gli3*, and *Hox10* genes downstream of *Sall4*, regulate femur and tibia development. In the autopod, we show that *Sall4* negatively regulates Hedgehog signaling, which allows for development of the most anterior digit. Collectively, our study illustrates genetic systems that regulate development of the proximal-anterior skeletal elements in hindlimbs.

KEYWORDS limb; *Sall4*; *Plzf*; proximal-anterior skeleton; Sonic Hedgehog-Gli3

LIMB development serves as an excellent system to study how progenitor cells develop into a functional system during embryonic development (Zeller *et al.* 2009; Tickle 2015). Specifically, limb progenitors arise in the distinct locations of the lateral plate mesoderm (LPM), and form paired protrusions covered by ectoderm, called the forelimb bud and hindlimb bud. Patterning, proliferation, and differentiation of limb progenitors during limb bud outgrowth results in the development of each skeletal element with a unique shape at a distinct location (Zeller *et al.* 2009). For instance, one thick long bone is formed in the most proximal region (stylopod), two long bones are formed in the middle region (zeugopod), and a varying number of smaller bones are formed in the distal region (autopod), depending on species. This basic skeletal pattern is evolutionarily conserved in animals with four limbs, providing a paradigm to study developmental mechanisms for stereotypical morphogenesis from progenitor cells (Zuniga 2015).

Recent studies provided genetic evidence that two signaling systems are established prior to or at the onset of limb bud outgrowth (Tao *et al.* 2017). These systems contribute to the development of the distal-posterior skeletal system and the proximal-anterior skeletal system (Li *et al.* 2014; Akiyama *et al.* 2015). The distal-posterior skeletal system depends

doi: https://doi.org/10.1534/genetics.120.303069
Manuscript received August 21, 2019; accepted for publication March 3, 2020; published Early Online March 10, 2020.
Supplemental material available at figshare: https://doi.org/10.25386/genetics.11918424.
[1]Present address: Department of Biochemistry and Molecular Biology, Mayo Clinic, Rochester, MN 55905.
[2]Corresponding author: Department of Genetics, Cell Biology and Development, University of Minnesota, Minneapolis, MN 55455. E-mail: kawak005@umn.edu

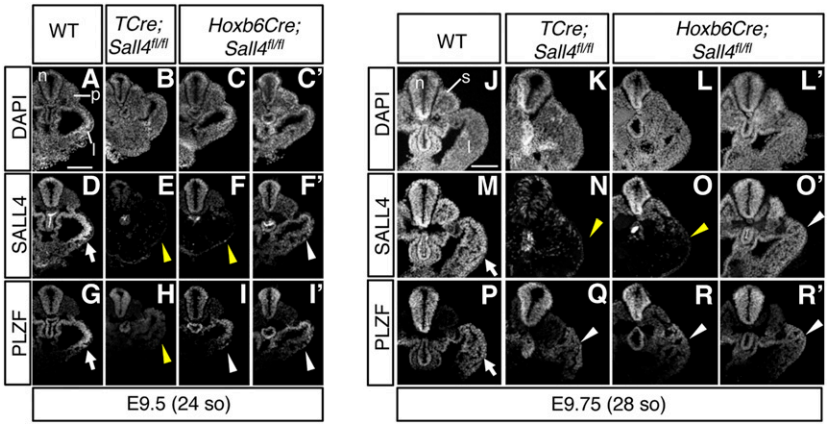

Figure 1 Comparison of SALL4 and PLZF immunoreactivities in WT, *TCre*; *Sall4*, and *Hoxb6Cre*; *Sall4* mutants. (A–I′) Confocal images of cross sections of E9.5 embryos at the level of the putative hindlimb-forming region (posterior to the last somite). DAPI (A–C′), SALL4 (D–F′), and PLZF (G–I′) immunofluorescence are shown. (J–R′) Confocal images of cross sections of E9.75 embryos at the hindlimb bud level. DAPI (J–L′), SALL4 (M–O′), and PLZF (P–R′) immunofluorescence are shown. White arrows point to normal expression. Yellow and white arrowheads point to substantial downregulation and moderate levels of downregulation, respectively. Bar, 100 μm. l, lateral plate mesoderm; n, neural tube; p, presomitic mesoderm; s, somites.

on Sonic Hedgehog (*Shh*), expressed in the posterior margin of the limb bud (Riddle *et al.* 1993; Tickle and Towers 2017). $Shh^{-/-}$ mice lack four posterior digits, termed as d2–d5, and the posterior zeugopod element (ulna in forelimbs and fibula in hindlimbs) (Chiang *et al.* 1996; Chiang *et al.* 2001; Kraus *et al.* 2001). Moreover, genetic lineage tracing studies demonstrated that cells expressing *Shh* and cells responding to SHH contribute to these distal-posterior skeletal elements (Ahn and Joyner 2004; Harfe *et al.* 2004). *Shh* regulates anterior-posterior patterning of limb buds and proliferative expansion of precursors that contribute to these distal-posterior skeletal elements (Zhu *et al.* 2008). In contrast, mechanisms underlying the development of the proximal-anterior skeletal elements, including the stylopod (humerus/femur), anterior zeugopod (radius/tibia), and anterior digits, are less clear.

With respect to the proximal-anterior skeletal elements, several studies have identified genes that regulate the development of these skeletal elements in a limb-type-specific manner. For instance, we have shown that *Sall4*, which encodes a zinc finger transcription factor (Sweetman and Munsterberg 2006; de Celis and Barrio 2009), functions as a critical regulator, specifically in hindlimbs (Akiyama *et al.* 2015). Conditional knockout (cKO) of *Sall4* using *TCre* resulted in the formation of a small cartilage aggregate at the position of the femur, and absence of the tibia (anterior zeugopod) and two or three anterior digits. Similar but milder defects were also observed in mutants lacking both *Irx3* and *Irx5* (referred to as *Irx3/5*) (Li *et al.* 2014). Moreover, simultaneous inactivation of all *Hox10* paralogs ($Hoxa10^{-/-}$; $Hoxc10^{-/-}$; $Hoxd10^{-/-}$; referred to as $Hox10^{-/-}$) results in the formation of a small cartilaginous femur without affecting the zeugopod and autopod elements (Wellik and Capecchi 2003). In the *Hox10* mutants, the forelimb skeleton exhibits only a minor phenotype, such as the lack of deltoid process in the humerus. It has been also demonstrated that combined function of *Plzf* and *Gli3* regulates the stylopod and zeugopod in hindlimbs (Barna *et al.* 2005). *Plzf* encodes a zinc finger transcription factor (Liu *et al.* 2016), and $Plzf^{-/-}$ mice exhibit a thin tibia (anterior zeugopod) and tri-phalangeal d1 in hindlimbs (Barna *et al.* 2000), which is considered to be a posterior transformation of anterior hindlimb elements. *Gli3* also encodes a zinc finger transcription factor involved in Hedgehog signaling (Hui and Angers 2011), and its mutation causes polydactyly, the development of multiple digits (Hui and Joyner 1993). Mouse embryos lacking both *Plzf* and *Gli3* exhibit severe defects in the stylopod and zeugopod of hindlimbs. Despite these proximal defects, the autopod is present and similar to $Gli3^{-/-}$ embryos; however, digit number is often reduced to four digits in $Plzf^{-/-}$; $Gli3^{-/-}$ hindlimbs (Barna *et al.* 2005). These functional studies provided evidence for genetic systems that regulate development of the proximal-anterior skeletal elements, but their exact relationship during development has not been elucidated.

Several other genes are also implicated in the proximal development. *Pbx* genes encode TALE- homeodomain proteins, and *Pbx1*, *Pbx2*, and *Pbx3* are expressed in the proximal part of the limb bud (Capellini *et al.* 2006; Capellini *et al.* 2011). The *Meis* genes also encode TALE-homeodomain proteins, and *Meis1*, *Meis2*, and *Meis3* are expressed in the proximal part of the limb bud. (Capdevila *et al.* 1999; Mercader *et al.* 1999; Mercader *et al.* 2000). The expression patterns of these genes have been used to assess the proximal identities of the limb bud (Tabin and Wolpert 2007; Mariani *et al.* 2008; Cooper *et al.* 2011; Rosello-Diez *et al.* 2011; Cunningham *et al.* 2013). Although $Pbx1^{-/-}$; $Pbx2^{-/-}$ embryos die around embryonic day (E) 9.5–10.5, $Pbx1^{-/-}$; $Pbx2^{+/-}$ embryos exhibited severe limb skeletal defects (Capellini *et al.* 2006). For instance, the digits and the fibula were missing and a rudimentary pelvic girdle was fused with a dysmorphic femur in the hindlimbs at E13.5, while forelimbs show slightly milder defects. However, the exact contributions of the entire *Pbx* family and *Meis* family in proximal development by triple mutants have not been reported.

Similar to the proximal development, anterior development is less understood compared to *Shh*-dependent posteior development (Tickle and Towers 2017). Genetic lineage tracing experiments demonstrated that the most

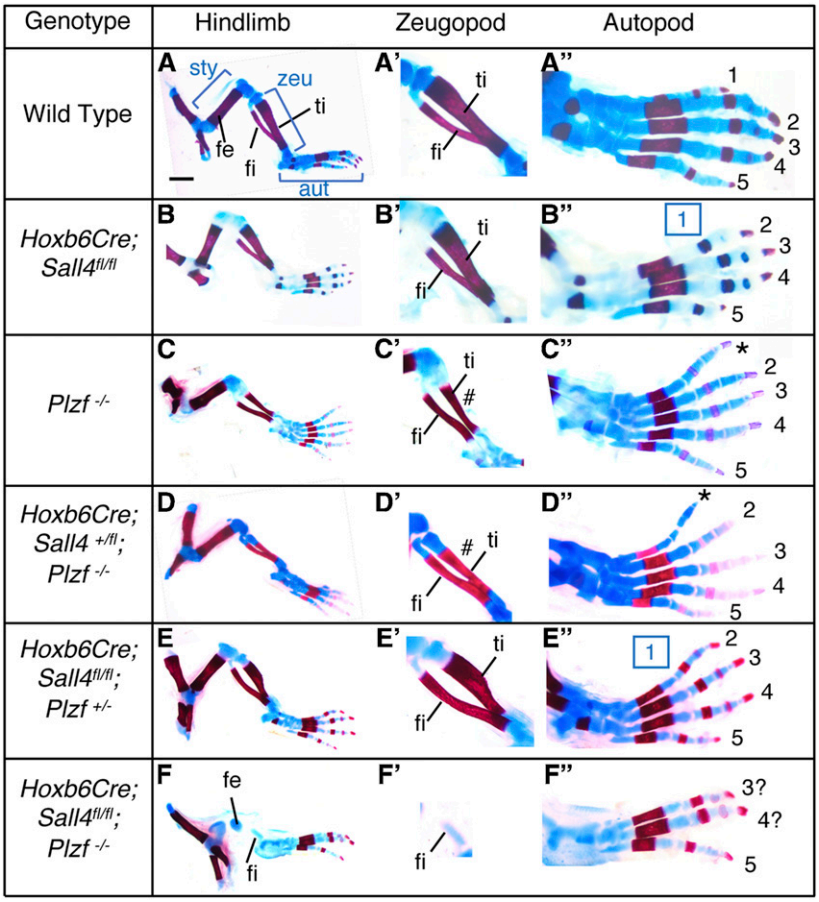

Figure 2 Combined functions of *Sall4* and *Plzf* regulate proximal-anterior skeletal development in the hindlimb. (A–F) Hindlimb skeleton of indicated genotypes. A'–F' show close up of the zeugopod region. A"–F" show close up of the autopod region. In the stylopod, a cartilage aggregate was formed in the position of the femur in the *Sall4*; *Plzf* dKO hindlimb (F). In the zeugopod, fibula-like thin tibia in $Plz^{f-/-}$ (C') and *Hoxb6Cre*; $Sall4^{+/fl}$; $Plzf^{-/-}$ (D') hindlimbs are indicated with #. In the autopod, 1–5 at the digit tip indicates each digit (A"–F"). Asterisk in C" and D" indicates triphalangeal digit 1. Loss of digit 1 in B" and E" are shown by boxed 1. The 3? and 4? in F" indicate two digits that appear to be digit 3 and 4, respectively. aut, autopod; fe, femur; fi, fibula; sty, stylopod; ti, tibia; zeu, zeugopod. Bar in A, 1 mm.

anterior digit, d1, is derived from cells that do not receive paracrine SHH signaling, indicating that d1 development is *Shh*-independent (Ahn and Joyner 2004; Harfe *et al.* 2004). A recent tudy also provided genetic evidence that excluding SHH signaling in the anterior of the limb bud is required for the development of d1 (Li *et al.* 2014). $Irx3/5^{-/-}$ hindlimbs lack d1, which is correlated with a reduced anterior domain free of SHH signaling in hindlimb buds. Similarly, *TCre*; *Sall4* cKO hindlimb buds also exhibit a smaller anterior domain that is free of SHH signaling in the hindlimb bud (Akiyama *et al.* 2015).

In this study, we expanded our previous study to understand the genetic mechanisms that regulate the development of the proximal-anterior skeletal system downstream of *Sall4*. By using a *Sall4* mutation with the *Hoxb6Cre* recombinase transgene, we provide genetic evidence that the combined function of *Sall4* and *Plzf* regulates the proximal-anterior skeletal system in hindlimbs. Our data show that *Sall4* and *Plzf* regulate expression of GLI3 and *Hox10* genes, and suggest that *Gli3*, *Plzf*, and *Hox10* genes, downstream of *Sall4*, regulates proximal skeletal development. Moreover, by reducing *Shh* gene dosage from *Sall4* mutants, we provide genetic evidence that support the notion that excluding SHH signaling is required for anterior digit development.

Materials and Methods

Mouse lines

This study used the following published mouse lines: $Gli3^{-}$ (Hui and Joyner 1993), *Hoxb6Cre* (Lowe *et al.* 2000), $Plzf^{-}$ (Barna *et al.* 2000), $Sall4^{fl}$ (Sakaki-Yumoto *et al.* 2006), Shh^{fl} (Dassule *et al.* 2000), and *TCre* (Perantoni *et al.* 2005). Animal breeding, timed mating, and dissection were performed according to the approval by the Institutional Animal Care and Use Committee of the University of Minnesota.

Skeletal staining and scoring

Alcian Blue/Alizarin Red skeletal staining was performed as previously described (Akiyama *et al.* 2015). Phenotypic evaluation shown in Figure 3 was performed by two or three independent individuals. Any inconsistencies in phenotype evaluation between individuals participating in scoring were discussed with a third individual and a final scoring decision was made.

In situ hybridization

Embryos were collected by timed mating and whole-mount *in situ* hybridization was performed as previously described (Akiyama *et al.* 2015). Three to five embryos per probe were examined.

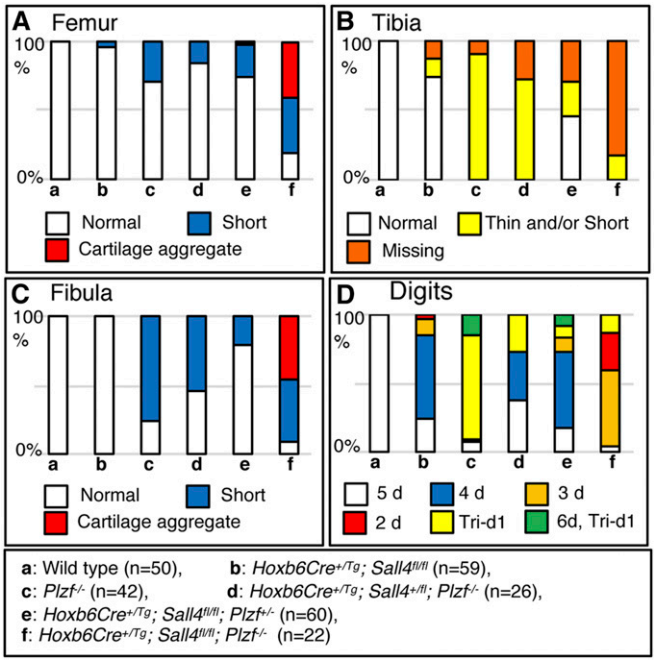

Figure 3 Graphic presentation of hindlimb skeletal phenotypes. Graphs showing defects in the (A) femur, (B) tibia, (C) fibula, and (D) digits. a–f represent the genotypes shown in a box below panels C and D. Number of limbs with each genotype are also shown in the same box. In D, 5d indicates 5 digits, and so on. Tri+d1 (yellow) indicates tri-phalangeal d1. 6d, Tri-d1 (green) indicates six digits with tri-phalangeal d1.

Immunofluorescence

Cryosections with 14-μm thickness were treated as previously described (Akiyama *et al.* 2015; Tahara *et al.* 2019). Primary antibodies against GLI3 (AF3690, 1:200; R&D Systems), PLZF (sc-22839, 1:100; Santa Cruz Biotechnology), and SALL4 (sc-101147, EE30, 1:300; Santa Cruz Biotechnology) were used. Alexa-Fluor-labeled secondary antibodies (1:500; Invitrogen, Carlsbad, CA) were used. Images were acquired by Zeiss LSM710 confocal microscope with Zen software.

Statistical analyses

Phenotypic evaluation of Sall4; Plzf allelic series: By using the scores, summarized in Supplemental Material, Table S1, we tested the hypotheses shown in Table S2 to evaluate whether mutations affect occurrence of the most severe phenotype of each skeletal element. For each hypothesis, we reduced the data table to values of interest, then condensed the table into the topic of interest over all genotypes. We then conducted the Fisher exact test on the entire table. For example, consider the following hypothesis: In the femur, the ratio of small cartilage aggregate in each genotype is different. We restrict the data to the data for the femur only, then for each genotype we count the cases of small cartilage aggregate as one category and all other cases as the other category. We are left with a two-by-six table (two categories, six genotypes) on which we conduct the Fisher exact test. If the *P*-value shows <0.05, it indicates that there is at least one pair of genotypes that exhibits a different ratio. Next, we performed the Fisher exact test between pairs of genotypes to identify which pairs have significant difference. More specifically, this is done by taking the two-by-six table used in the previous Fisher exact test and looking at the columns corresponding to the two genotypes of interest. As a result, we have a two-by-two table which we use to conduct the Fisher exact test. Because of the 15 combinations of paired comparisons, we used a Bonferroni correction of significance value of $0.05/15 = 0.00333$. Therefore, if a *P*-value between a given pair is <0.00333, the tested pair has significant differences in the ratio of occurrence of specific phenotype (McDonald 2008a,b; Agresti 2012).

Digit 1 rescue experiment: We tested the hypotheses in Table S4 by using the Fisher exact test to determine statistical significance (Figure 8D). Similar to previous analysis, the data for the phenotype was collapsed into two categories: five digits, and all other cases. We thus obtain a two-by-two table on which we conduct the Fisher exact test.

Ratio of the Gli1 expression domain: The *Gli1* expression domain in dorsal view images of hindlimb buds was analyzed by measuring hindlimb bud area and *Gli1*-expressing area using FIJI (Figure 8H). To confirm the stained domain with weak signals, signal enhancement by FIJI was performed before measurement. Four individuals independently performed measurements, which led to similar results. We used one-way ANOVA and Tukey's test on the three genotypes to determine significance of differences between the genotypes.

Data availability

All mouse lines and plasmid DNA are available upon request. Figure S1 shows SALL4 expression in wild-type (WT) and *TCre*; *Sall4* cKO embryos at E8.5. Figure S2 shows forelimb skeletons of *Sall4*; *Plzf* allelic series. Figure S3 shows GLI3 immunofluorescence on WT and $Gli3^{-/-}$ hindlimb buds. Figure S4 shows the hindlimb autopod of *Sall4*; *Gli3* allelic series. Table S1 contains summary of hindlimb skeletal phenotypes. Table S2 shows statistical examination of *Sall4*; *Plzf* skeletal phenotypes. Table S3 shows summary of femur defects in *Sall4*; *Gli3* allelic series. Table S4 shows statistical examination of *Shh* contributions to the loss of digit phenotype in hindlimbs. Supplemental material available at figshare: https://doi.org/10.25386/genetics.11918424.

Results

Differences of SALL4 and PLZF expression in TCre; Sall4 and Hoxb6Cre; Sall4 mutants

Our previous *Sall4* cKO study showed that *Sall4* deletion by two Cre recombinase transgenic lines resulted in notably different hindlimb phenotypes (Akiyama *et al.* 2015).

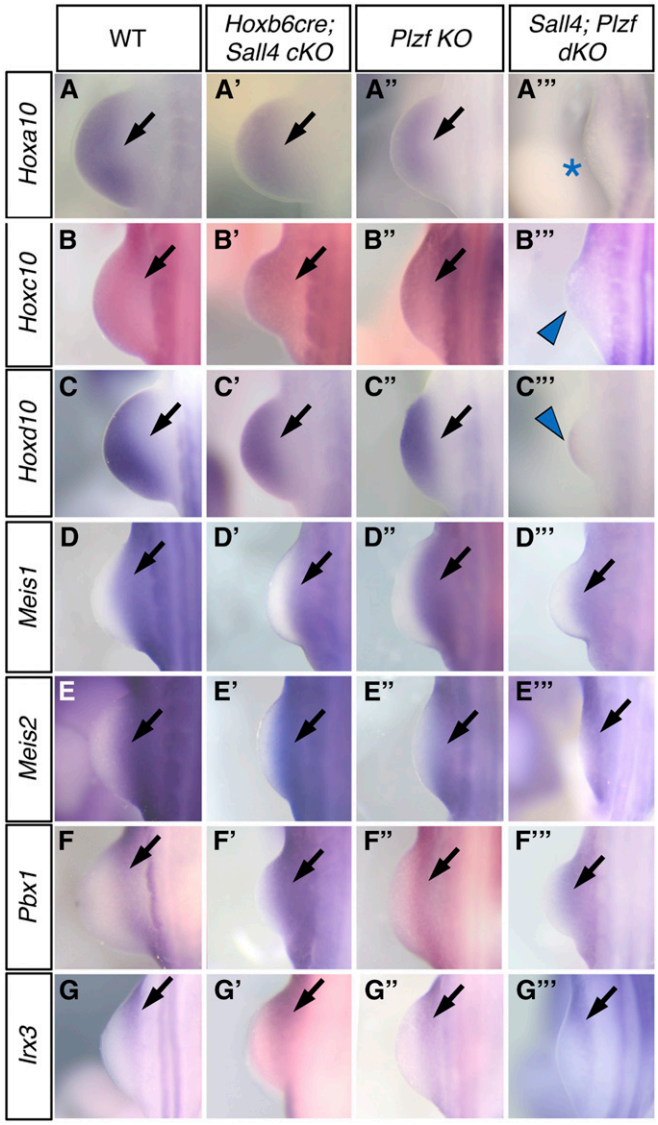

Figure 4 Altered *Hox10* expression pattern in *Sall4*; *Plzf* dKO hindlimb buds. (A–C′″) Expression pattern of *Hoxa10* (A–A′″), *Hoxc10* (B–B′″), and *Hoxd10* (D–D′″) in hindlimb buds of indicated genotypes at E10.5. *Hoxa10* was undetectable in *Sall4*; *Plzf* dKO hindlimb buds (A′″). Faint expression of *Hoxc10* (B′″) and *Hoxd10* (C′″) was detected at the anterior margin and distal margin of hindlimb buds, respectively. Note that *Hoxc10* expression in somites are detectable in *Sall4*; *Plzf* dKO hindlimb buds. (D–G′″) Expression pattern of *Meis1* (D–D′″), *Meis2* (E–E′″), *Pbx1* (F–F′″), and *Irx3* (G–G′″) in hindlimb buds of indicated genotypes at E10.5. These genes are expressed in the proximal part of hindlimb buds with each genotype. Black arrows point to expression in WT and those similar to WT. Blue arrowheads and asterisks indicate weak expression and undetectable expression, respectively.

Specifically, *TCre*-mediated inactivation of *Sall4* during gastrulation caused severe defects of the femur, tibia, and anterior digits (d1–d3). In contrast, *Sall4* deletion in the LPM before limb outgrowth by *Hoxb6Cre* resulted in a loss of only the most anterior digit (d1) in most of affected mutants. *Sall4* is highly expressed in gastrulating embryos and in the posterior part of postgastrulation embryos (Kohlhase *et al.* 2002; Tahara *et al.* 2018), raising the possibility that differences in remaining SALL4 protein might account for the difference between *TCre*- and *Hoxb6Cre*-mediated cKO phenotypes.

Our previous study also showed that *Plzf* expression is downstream of *Sall4* in the nascent hindlimb bud at E9.75 (27/28 somite stage) (Akiyama *et al.* 2015), suggesting that *Plzf* may contribute to the differences of the phenotypes. Therefore, we examined immunoreactivities of SALL4 and PLZF in WT, *TCre*; *Sall4* cKO, and *Hoxb6Cre*; *Sall4* cKO embryos. At E9.5 (24-somite stage), just prior to hindlimb bud outgrowth, we observed efficient deletion of SALL4 in the LPM, presomitic mesoderm, and neural tube in the *TCre*; *Sall4* mutants, consistent with broad activity of *TCre* in mesodermal progenitors and neuromesodermal progenitors (Akiyama *et al.* 2015; Tahara *et al.* 2019) ($n = 3$, Figure 1, A, B, D, and E). PLZF expression in *TCre*; *Sall4* mutants were also substantially downregulated ($n = 3$, Figure 1, G and H). In contrast, SALL4 deletion in LPM was variable in *Hoxb6Cre*; *Sall4* cKO embryos, consistent with our previous observation of variable *Isl1* inactivation by *Hoxb6Cre* (Itou *et al.* 2012). For example, SALL4 expression was substantially reduced in some of the *Hoxb6Cre*; *Sall4* cKO embryos ($n = 3$, Figure 1, C and F), but a fraction of the cKO embryos showed evident SALL4 expression that were weaker than those in WT embryos ($n = 1$, Figure 1, C' and F'). In *Hoxb6Cre*; *Sall4* cKO embryos PLZF expression was substantially stronger than those of *TCre*; *Sall4* mutants ($n = 4$, Figure 1, G, H, I, and I'').

We also examined embryos at E9.75 (28-somite stage), soon after hindlimb bud outgrowth begins. SALL4 deletion was efficient in the hindlimb bud of *TCre*; *Sall4* mutants ($n = 3$, Figure 1, J, K, M, and N), but was variable in *Hoxb6Cre*; *Sall4* mutants ($n = 3$, Figure 1, L and O; $n = 1$, Figure 1, L' and O'). PLZF expression in all mutants was detectable but weaker than that of WT (Figure 1, P–R'), indicating that SALL4 in the nascent limb bud partially contributes to PLZF expression. In addition to these stages just prior to and after hindlimb bud outgrowth, we also examined SALL4 immunoreactivities at E8.5 in WT and *TCre*; *Sall4* mutants. At this stage, *Hoxb6Cre*-dependent recombination has not occurred in the LPM (Akiyama *et al.* 2015), and embryos have not developed hindlimb forming region. SALL4 expression was detected in a speckled manner in the forelimb-forming region (posterior to the seventh somite level) in *TCre*; *Sall4* mutant, compared to WT embryos ($n = 3$, Figure S1). These results indicate efficient deletion of SALL4 before hindlimb outgrowth in *TCre*; *Sall4* and variable deletion in *Hoxb6Cre*; *Sall4* mutants, and suggest that the phenotypic difference may involve a difference of PLZF downregulation at E9.5.

Combined functions of Sall4 and Plzf regulates the development of proximal-anterior skeletons

To test the hypothesis that functional interaction of *Sall4* and *Plzf* regulates development of the proximal-anterior skeletal elements, we simultaneously inactivated *Plzf* on the *Hoxb6Cre*; *Sall4* cKO background. We found surprisingly similar phenotypes of *Hoxb6Cre*; *Sall4*$^{fl/fl}$; *Plzf*$^{-/-}$ [hereafter referred to as *Sall4*; *Plzf* double knockout (dKO)] hindlimbs

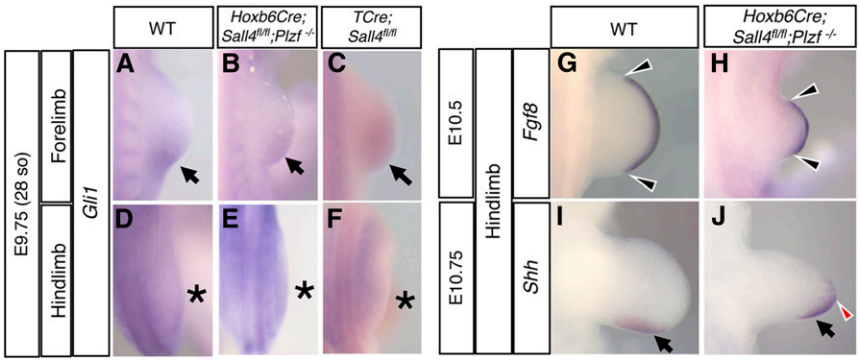

Figure 5 Precocious activation of Hedgehog signaling was not detected in *Sall4*; *Plzf* dKO hindlimb buds. (A–F) Dorsal views of *Gli1* expression in the forelimb bud (A–C) and hindlimb bud (D–F) in wild-type, *Sall4*; *Plzf* dKO, and *TCre*; *Sall4* cKO embryos at E9.75. Arrows point to *Gli1* expression in forelimb buds and asterisks indicate a lack of *Gli1* expression in hindlimb buds. (G and H) Dorsal view of hindlimb buds hybridized with *Fgf8* probe at E10.5. Arrowheads point to the anterior and posterior edges of *Fgf8*-expressing apical ectodermal ridge. (I and J) Dorsal views of hindlimb buds hybridized with *Shh* probe at E10.75. Black arrows point to *Shh* expression in the posterior mesenchyme, and red arrowhead points to *Shh* expression extended to the distal-middle part of the hindlimb bud.

to *TCre*; *Sall4* cKO hindlimbs (Figure 2, Figure 3, and Table S1) (Akiyama *et al.* 2015). Specifically, the femur exhibited either a small cartilage aggregate or was noticeably short. The tibia was missing in most of the mutants, and the fibula exhibited either a small cartilage aggregate or short. Two or three anterior digits were missing in most of mutants. In contrast, *Hoxb6Cre*; *Sall4*$^{+/fl}$; *Plzf*$^{-/-}$ mutants exhibited similar phenotype to *Plzf*$^{-/-}$ mutants, such as thin tibia and triphalangeal d1 (Figure 2, C–D") (Barna *et al.* 2000). Similarly, *Hoxb6Cre*; *Sall4*$^{fl/fl}$; *Plzf*$^{+/-}$ mutants exhibited similar phenotype to *Hoxb6Cre*; *Sall4* cKO mutants, such as loss of d1 (Figure 2, B–B" and Figure 2, E–E"). In contrast to these hindlimb defects, in most mutants, forelimbs developed without noticeable defects in the stylopod and zeugopod (Figure S2). A small fraction of the *Plzf*$^{-/-}$ genotype was associated with triphalangeal thumb and an anterior extra digit, as previously reported (Barna *et al.* 2000). To further examine skeletal defects in more detail, we quantitatively assessed defects in each skeletal elements (Figure 3 and Table S2). In this analysis, we defined a "short" element as an element with less than roughly two-thirds of the length of the element in age-matched WT. Statistical examination of defects in each skeletal elements demonstrated that *Sall4;Plzf* dKO mutants exhibit distinct skeletal defects in the stylopod, zeugopod, and the digit loss compared to other combinations of *Sall4;Plzf* mutant genotypes (Table S2). These results support the notion that the combined function of *Sall4* and *Plzf* regulates development of the proximal-anterior skeletal elements in hindlimb. The results also provide evidence that the more severe skeletal defects of early loss of *Sall4* by *TCre*, compared to later loss by *Hoxb6Cre*, may be derived from the loss of PLZF expression when *Sall4* is deleted earlier.

Expression pattern of Hox10 genes, but not other proximal markers, are downregulated in Sall4; Plzf dKO hindlimb buds

A prior genetic study has demonstrated that simultaneous inactivation of all *Hox10* paralogs (*Hoxa10*, *c10*, *d10*) caused defects in the femur (Wellik and Capecchi 2003). Our previous study also showed that *Hox10* genes are downregulated, but not abolished, in *TCre*; *Sall4* cKO hindlimb buds (Akiyama *et al.* 2015). Consistent with these studies, expression of *Hox10* genes are severely downregulated in *Sall4*; *Plzf* dKO hindlimb buds. Specifically, expression of *Hoxa10* (n = 3) became undetectable and expression of *Hoxc10* (n = 5) was faint in *Sall4*; *Plzf* dKO hindlimb buds (Figure 4, A and A" and Figure 4, B and B"'). In addition, weak *Hoxd10* expression became restricted to the distal margin of *Sall4*; *Plzf* dKO hindlimb buds (n = 3, Figure 1, C and C"'). In contrast, expression of these genes in *Hoxb6Cre*; *Sall4* cKO and *Plzf*$^{-/-}$ hindlimb buds appear to be similar pattern to that of WT (n = 4 for *Hoxa10*, n = 6 for *Hoxc10*, and n = 5 for *Hoxd10*, Figure 4, A–A", B–B", and C–C").

We also examined expression patterns of other proximal markers. Expression of *Meis1*, *Meis2*, and *Pbx1* was detected in the proximal part of *Sall4*; *Plzf* dKO hindlimb buds (n = 3 for each gene, Figure 3, D and D"', E and E"', and F and F"'), in addition to *Hoxb6Cre*; *Sall4* cKO and *Plzf*$^{-/-}$ hindlimb buds (at least three for each gene and each genotype, Figure 3, D–D", E–E", and F–F"). Moreover, the expression pattern of *Irx3* was detected in the proximal part of the *Sall4*; *Plzf* dKO hindlimb buds, similar to hindlimb buds with other genotypes (n = 3 for each genotype, Figure 3, G–G"'). These results support the idea that *Hox10* genes functionally mediate femur development, downstream of combined functions of *Sall4* and *Plzf*. The results also suggest that the *Irx3/5* pathway is parallel to the *Sall4-Plzf* pathway.

The Shh-expression domain is distally extended in Sall4; Plzf dKO hindlimb buds

In addition to the analysis of *Hox* gene expression patterns, we also tested whether precocious activation of Hedgehog signaling, which is known to cause defects of limb development (Butterfield *et al.* 2009; Zhulyn *et al.* 2014), is involved in the *Sall4*; *Plzf* dKO phenotype. Precocious activation of Hedgehog signaling by genetically removing negative regulator *Ptch1* causes ectopic expression of *Gli1*, a target of Hedgehog signaling, in limb buds prior to expression of *Shh* (Zhulyn *et al.* 2014). *Gli1* was not induced in *Sall4*; *Plzf* dKO hindlimb buds at E9.75 before expression of *Shh*, similar to WT hindlimb buds (Figure 5, A, B, D, and E). Similarly, *Gli1* was not induced in *TCre*; *Sall4* cKO hindlimb bud at E9.75 (Figure 5, C and F).

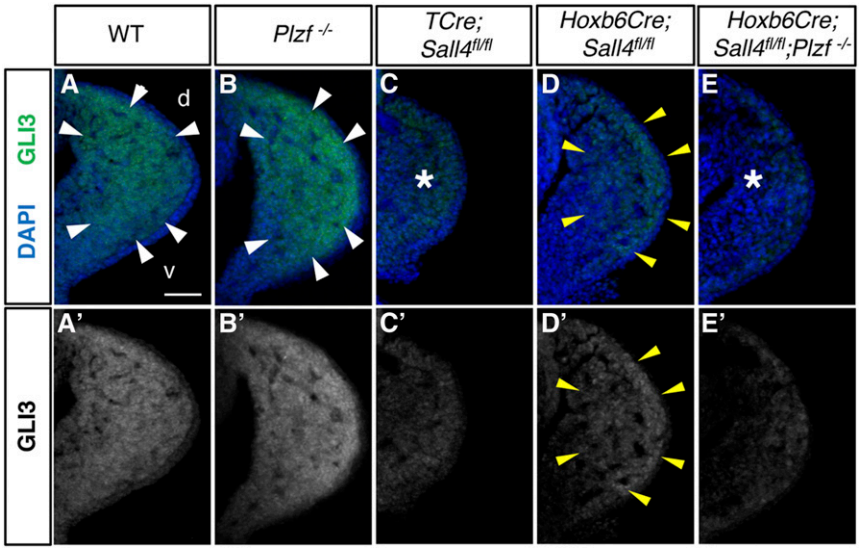

Figure 6 Combined functions of *Sall4* and *Plzf* regulates GLI3. Confocal images of cross sections of hindlimb buds at E10.5 with the WT (A and A'), *Plzf*$^{-/-}$ (B and B'), *TCre*; *Sall4*$^{fl/fl}$ (C and C'), *Hoxb6Cre*; *Sall4*$^{fl/fl}$ (D and D'), and *Hoxb6Cre*; *Sall4*$^{fl/fl}$; *Plzf*$^{-/-}$ (E and E') genotypes. In A–E, GLI3 (green) and DAPI (blue) stainings are overlayed. In A'–E' only GLI3 expression is shown in black/white for the better presentation. White arrows point to strong expression in WT (A) and *Plzf*$^{-/-}$ hindlimb buds (B). Yellow arrowheads in D and D' point to moderate downregulation. Asterisks in C, C', E, and E' indicate substantial downregulation of GLI3 expression. For better presentation of GLI3 expression, asterisks are not introduced in C' and E'. d, dorsal; v, ventral. Bar in A, 50 μm.

Precocious activation of Hedgehog signaling also causes failure to establish the *Fgf8*-expressing apical ectodermal ridge and a failure to localize *Shh*-expression domain in the posterior mesenchyme (Butterfield *et al.* 2009; Zhulyn *et al.* 2014). In *Sall4*; *Plzf* dKO hindlimb buds, expression of *Fgf8* was detected in the apical ectodermal ridge (Figure 5, G and H). Expression pattern of *Shh* extends distally, while the expression domain remains in the posterior mesenchyme in *Sall4*; *Plzf* dKO hindlimb buds (Figure 5, I and J). Therefore, the *Sall4*; *Plzf* dKO hindlimb buds did not exhibit the precocious activation of Hedgehog signaling observed in *Ptch1* cKO limb buds.

A previous study of *Irx3/5*$^{-/-}$ hindlimbs suggests that distally-extended Hedgehog signaling may negatively affect the development of the anterior skeletal elements (Li *et al.* 2014). Therefore, we attempted to test whether genetically removing one allele of *Shh* can rescue the long bone defects in *Sall4*; *Plzf* dKO hindlimbs. However, timed mating of *Sall4*$^{fl/fl}$; *Plzf*$^{+/-}$; *Shh*$^{+/fl}$ females and *Hoxb6Cre*$^{Tg/Tg}$; *Sall4*$^{fl/fl}$; *Plzf*$^{+/-}$ males generated no embryos with the *Hoxb6Cre*$^{+/tg}$; *Sall4*$^{fl/fl}$; *Plzf*$^{-/-}$; *Shh*$^{+/fl}$ genotype at E14.5 (out of 13 females, 56 embryos recovered and 30 embryos absorbed), presumably due to lethality. In summary, distal expansion of *Shh* expression domain in *Sall4*; *Plzf* dKO hindlimb bud may also contribute to anterior skeletal defects.

Combined function of Sall4 and Plzf regulates GLI3

A genetic study in mice has demonstrated that *Plzf*$^{-/-}$; *Gli3*$^{-/-}$ mutants exhibit severe defects of the stylopod and zeugopod in hindlimbs (Barna *et al.* 2005), which is similar to defects observed in *TCre*; *Sall4* cKO and *Sall4*; *Plzf* dKO mutants (Akiyama *et al.* 2015). The similar phenotype raises the possibility that *Gli3* is involved in the defects of *Sall4*; *Plzf* dKO hindlimbs. Therefore, we examined GLI3 immunoreactivities. GLI3 was detected in *Plzf*$^{-/-}$ hindlimb buds, similar to WT hindlimb buds (n = 3, Figure 6, A and A', n = 3, Figure 6, B and B', Figure S3). In *Hoxb6Cre*; *Sall4* cKO hindlimbs, GLI3 expression was reduced compared to WT hindlimb buds (n = 3, Figure 6, D and D'). In both *TCre*; *Sall4* cKO and *Sall4*; *Plzf* dKO hindlimb buds, GLI3 was substantially downregulated (n = 3, Figure 6, C and C', n = 3, Figure 6, E and E'). These results indicate that GLI3 expression is downstream of the combined function of *Sall4* and *Plzf*.

Proximal hindlimb skeleton develops in the absence of Sall4 and Gli3

The downregulation of GLI3 in *Sall4*; *Plzf* dKO hindlimb buds raises the possibility that *Sall4-Gli3* interaction regulates femur development. To test this possibility, we simultaneously inactivated *Gli3* on the *Hoxb6Cre*; *Sall4* cKO background (Figure 7, Figure S4). As *Gli3*$^{-/-}$ mutants die perinatally (Johnson 1967; Hui and Joyner 1993), we examined hindlimbs at E13.5–E16.5 stages. In *Hoxb6Cre*; *Sall4*$^{fl/fl}$; *Gli3*$^{-/-}$ dKO mutants, the femur elongated (n = 10/12, Figure 7F, and Table S3), and do not resemble the ball-like cartilage aggregate in *Sall4*; *Plzf* dKO hindlimbs (Figure 2F). A fraction of *Hoxb6Cre*; *Sall4*$^{fl/fl}$; *Gli3*$^{+/-}$ femur exhibited a very thin center region (n = 4/24, Figure 7E, and Table S3). Two hindlimbs from the same *Hoxb6Cre*; *Sall4*$^{fl/fl}$; *Gli3*$^{-/-}$ dKO embryo exhibited a small cartilage aggregate in the stylopod, which may be caused by earlier recombination than other embryos due to the variable nature of recombination by *Hoxb6Cre* (Itou *et al.* 2012). The femur of other *Hoxb6Cre*; *Sall4*$^{fl/fl}$; *Gli3*$^{-/-}$ dKO embryos elongated, and a fraction of these mutants exhibited a lack of Alcian Blue staining in the center of the femur (n = 4/12, Figure 7F, and Table S3). Similar to the nascent limb bud at E9.75 (Figure 1), PLZF expression in *Hoxb6Cre*; *Sall4*$^{fl/fl}$ and *Hoxb6Cre*; *Sall4*$^{fl/fl}$; *Gli3*$^{-/-}$ dKO hindlimb buds was detectable but lower than that of WT and *Gli3*$^{-/-}$ hindlimb buds (n = 3 for each genotype, Figure 7, G–N). Therefore, combined function of *Sall4* and *Gli3* does not regulate femur development compared to the combined function of *Sall4* and *Plzf*.

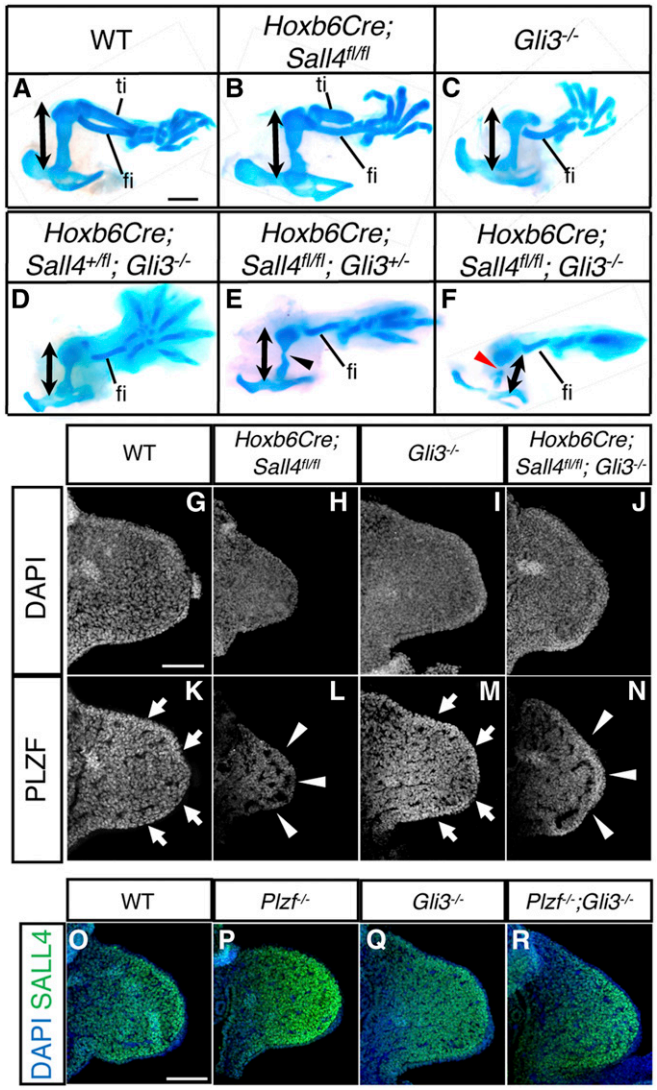

Figure 7 The femur develops in *Sall4*; *Gli3* dKO mutants and *Sall4* is upstream of *Plzf*; *Gli3* interaction. (A–F) Alcian blue-stained hindlimb skeleton of E14.5 embryos with indicated genotypes. Double arrowheads indicate the elongated developing femur. Numbers of samples with each genotype are shown in Table S3. The autopod region is shown in Figure S4. Black (E) and red (F) arrowheads point to thin regions and discontinuous Alcian Blue staining, respectively, in the center of the femur. Bar in A, 1 mm. (G–N) Confocal images of cross sections of hindlimb buds of indicated genotypes. DAPI staining (G–J) and PLZF expression (K–N) are shown. Arrows and arrowheads point to normal expression and moderate levels of downregulation, respectively. Bar in G, 100 μm. (O–R) Confocal images of cross sections of hindlimb buds of WT (O), $Plzf^{-/-}$ (P), $Gli3^{-/-}$ (Q), and $Plzf^{-/-}$; $Gli3^{-/-}$ (R) embryos at E10.5. SALL4 expression (green) and DAPI staining (blue) are shown. Strong SALL4 expression was detected in hindlimb buds with all genotypes. fi, fibula; ti, tibia. Bar in O, 100 μm.

Sall4 is upstream of Plzf and Gli3

Given the reported severe proximal skeletal defects in $Plzf^{-/-}$; $Gli3^{-/-}$ hindlimbs (Barna *et al.* 2005), our results suggest that *Gli3* (downstream of *Sall4* and *Plzf*) and *Plzf* could regulate femur development. It is also possible that *Plzf* and *Gli3* cooperate to regulate *Sall4*, and combined function of *Sall4*, *Plzf* and *Gli3* regulates femur development. To test whether the $Plzf^{-/-}$; $Gli3^{-/-}$ phenotype involves *Sall4* function, we examined SALL4 expression. Immunofluorescence analysis showed that SALL4 is expressed in $Plzf^{-/-}$; $Gli3^{-/-}$ hindlimb buds ($n = 3$), similar to WT ($n = 3$), $Plzf^{-/-}$ ($n = 3$), and $Gli3^{-/-}$ ($n = 3$) hindlimb buds (Figure 7, O–R). This result, combined with other results obtained in this study, indicates that *Sall4* expression before hindlimb bud outgrowth is upstream of *Plzf* in the nascent hindlimb bud, and *Sall4* and *Plzf* regulates *Gli3* in hindlimb buds. These results also suggest that the downregulation of *Plzf* and *Gli3* contributes to the defects of the femur and tibia in *TCre*; *Sall4* cKO, and that *Sall4* does not act alone in the development of these skeletal elements.

Sall4 contributes to the development of anterior digit through negative regulation of Hedgehog signaling during hindlimb bud outgrowth

Shh expression domain is distally extended in *Sall4*; *Plzf* dKO hindlimb buds (Figure 5). A previous study provided evidence that SHH signaling negatively regulates d1 development and that excluding SHH signaling from the anterior portion of limb buds by *Irx3/5* is required for d1 development (Li *et al.* 2014). Therefore, we tested whether *Sall4* negatively regulates SHH signaling for d1 development by removing one allele of *Shh* from the *Hoxb6Cre*; *Sall4* cKO background. Approximately 52% and 16% of *Hoxb6Cre*; *Sall4* cKO hindlimbs possess four and three digits, respectively, and 32% possess five digits at E13.5–E15.5 (Figure 2, Figure 8, A–D, and Table S4). Removing one allele of *Shh* from the *Hoxb6Cre*; *Sall4* cKO background resulted in increased ratio of hindlimbs with five digits (63%, Figure 8, C and D). In addition, a fraction of hindlimbs exhibited small-digit-like spike in the position of d1 (10.4%, marked by an asterisk in Figure 8C). At the molecular level, *Gli1* expression domain was expanded toward the anterior in *Hoxb6Cre*; *Sall4* cKO hindlimb buds compared to WT. Removing one allele of *Shh* partially rescued expanded *Gli1* expression domain in *Hoxb6Cre*; *Sall4* cKO hindlimb buds (Figure 8, E–H). These results support the notion that increased SHH signaling toward the anterior limb buds contributes to loss of d1 in *Hoxb6Cre*; *Sall4* cKO hindlimbs, and suggest that *Sall4* negatively regulates SHH signaling in the anterior region of hindlimb buds.

Discussion

Limb progenitor cells develop into all the appendicular skeletal elements, which can be divided into distal-posterior and proximal-anterior elements (Tao *et al.* 2017). Development of the distal-posterior skeletons depends on SHH signaling, which has been extensively studied (Anderson *et al.* 2012; Zuniga 2015; Lopez-Rios 2016; Delgado and Torres 2017; Tickle and Towers 2017). In this study, we demonstrated that SALL4 expression prior to hindlimb bud outgrowth regulates subsequent development of the stylopod and anterior

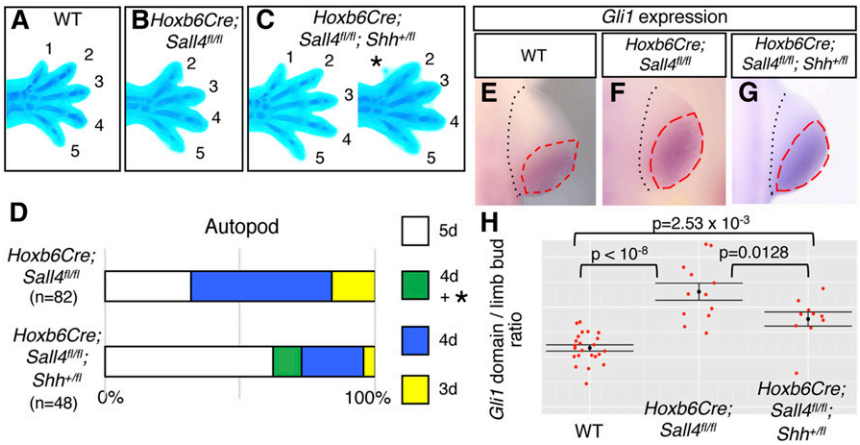

Figure 8 *Sall4* contributes to the development of anterior digit through negative regulation of Hedgehog signaling. (A–C) Alcian blue-stained autopod of WT (A), *Hoxb6Cre*; *Sall4*$^{fl/fl}$ (B), and *Hoxb6Cre*; *Sall4*$^{fl/fl}$; *Shh*$^{+/fl}$ (C) mutants at E14.5. Numbers 1–5 indicate each digit, asterisk indicates a protrusion in the anterior part of the autopod in *Hoxb6Cre*; *Sall4*$^{fl/fl}$; *Shh*$^{+/fl}$ mutants. (D) Graphic representation of digit phenotypes in *Hoxb6Cre*; *Sall4*$^{fl/fl}$ and *Hoxb6Cre*; *Sall4*$^{fl/fl}$; *Shh*$^{+/fl}$ mutants. 4d + * indicates 4 digits plus a protrusion, shown in panels C. (E–G) Whole-mount *Gli1 in situ* hybridization images of WT (E), *Hoxb6Cre*; *Sall4*$^{fl/fl}$ (F), and *Hoxb6Cre*; *Sall4*$^{fl/fl}$; *Shh*$^{+/fl}$ (G) hindlimb buds at E10.5. Black and red dotted lines line the border of the limb bud and *Gli1* expression domain, respectively. (H) Graphic representation of the ratio of *Gli1* expression domain over the limb bud area in hindlimb buds with each genotype. *P*-values are shown in the graph.

zeugopod in hindlimbs. Moreover, by individual and simultaneous knockout of *Sall4*, *Plzf*, *Gli3* and *Shh*, our results also suggest that distinct genetic mechanisms regulate the development of the stylopod, zeugopod, and autopod within the proximal-anterior skeleton (Figure 9A). Our data with *Sall4*, together with a previous study of *Irx3/5* (Li *et al.* 2014), also support the notion that the proximal-anterior programs and the *Shh*-dependent distal-posterior program antagonize during the outgrowth period (Figure 9B).

Sall4 functions for hindlimb development prior to the onset of hindlimb bud outgrowth

Our analysis of SALL4 and PLZF immunoreactivities indicated an early onset of gene regulation for the development of proximal-anterior skeletal elements in the hindlimb. In both *TCre*; *Sall4* and *Hoxb6Cre*; *Sall4* mutants, SALL4 immunoreactivities were downregulated by E9.5 (24-somite stage), prior to hindlimb bud outgrowth. However, PLZF immunoreactivities exhibited differences between these mutants. PLZF downregulation was more substantial in *TCre*; *Sall4* mutants than *Hoxb6Cre*; *Sall4* mutants. In contrast, in developing hindlimb buds (at E9.75 and E10.5), PLZF was only partially downregulated in both *TCre*; *Sall4* mutants and *Hoxb6Cre*; *Sall4* mutants. These differences in PLZF downregulation suggests two modes of PLZF regulation by *Sall4*. Prior to hindlimb bud outgrowth *Sall4* is required for PLZF expression in the hindlimb progenitors in the LPM (Figure 9B). After the hindlimb bud starts outgrowth, *Sall4* partially contributes to PLZF expression and another gene(s) may also regulate PLZF. The *Sall4* regulation of *Plzf* before hindlimb bud outgrowth supports our previous notion that genetic programs for the development of hindlimb skeletal elements start prior to or at the onset of hindlimb initiation (Li *et al.* 2014; Akiyama *et al.* 2015; Tao *et al.* 2017).

TCre; *Sall4* mutant phenotypes exhibit striking differences between the forelimbs and hindlimbs, which may involve differences of timing in forelimb and hindlimb specification. Forelimb development proceeds ~0.5 days prior to hindlimb development in mouse embryos. At E8.5, *Tbx5* expression in the forelimb progenitors is induced at the eight-somite stage in the LPM and is essential for forelimb specification (Agarwal *et al.* 2003; Zhao *et al.* 2009; Cunningham *et al.* 2013), and forelimb bud outgrowth starts around E9.0 at the 7–12 somite level. Our immunofluorescence analysis showed that SALL4 was present in the forelimb-forming region of *TCre*; *Sall4* cKO embryos in a speckled manner at E8.5, indicating that some of forelimb progenitor cells maintain detectable levels of SALL4 at this stage. Similar to our recent analysis of the posterior end of the *TCre*; *Sall4* mutant embryos (Tahara *et al.* 2019), SALL4 protein may be stable and persist after deletion of the *Sall4* gene. Moreover, *Hoxb6Cre*-dependent recombination occurs after E8.5 and *Hoxb6Cre* does not recombine in cells that contribute to the proximal-anterior part of forelimb buds (Lowe *et al.* 2000; Akiyama *et al.* 2015). Because of the early timing of forelimb specification, the forelimb progenitors are unlikely affected by the *Sall4* cKO method. Moreover, our recent study using *Sall4-CreER* mouse line showed that *Sall4* lineage contribution to forelimb buds and hindlimb buds is notably different (Tahara *et al.* 2018). When tamoxifen-dependent labeling of the *Sall4* lineage is done at E8.5 (recombination would occur at E9.0–E9.5), *Sall4* lineage contribution is already low and sparse in forelimb buds, but strong in hindlimb buds. The difference of *Sall4* lineage contribution also suggests that the cKO strategy may not target *Sall4* early enough to affect forelimb development.

In addition to the difference of timing discussed above, *Sall4* might genetically interact with hindlimb-specific transcription factors, such as *Tbx4* (Naiche and Papaioannou 2007) and *Pitx1* (Lanctot *et al.* 1999; Logan and Tabin 1999; Szeto *et al.* 1999), to modulate genetic systems commonly operating in forelimb buds and hindlimb buds (Schneider and Shubin 2013; Sears *et al.* 2015; Jain *et al.* 2018).

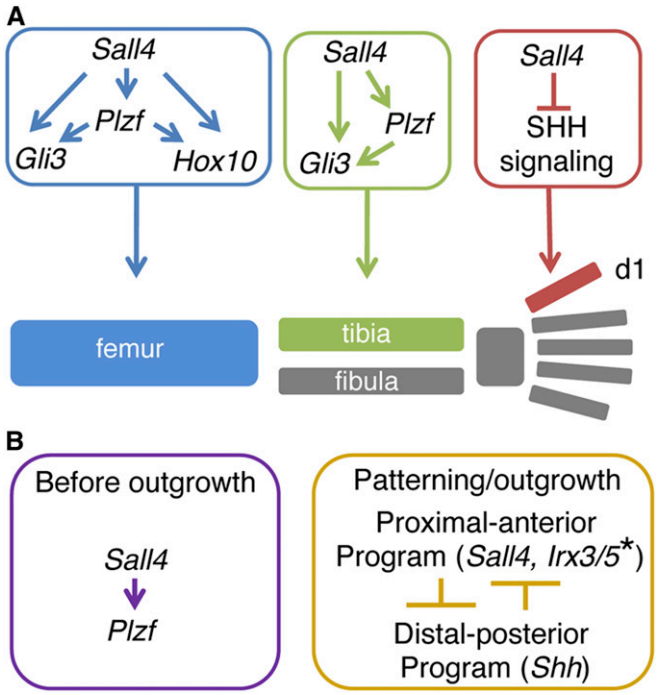

Figure 9 Model of genetic pathway for the development of anterior-proximal skeletal elements. (A) Relationship of *Sall4* with known regulators of the development of each skeletal element are depicted. (B) Schematics of regulation in two distinct temporal windows (before hindlimb outgrowth and during outgrowth/patterning phase). Asterisk indicates published data from Li *et al.* (2014). For further detail, please see the *Discussion*.

Genetic cascades for the development of stylopod and zeugopod

Our results provided evidence that within the proximal-anterior skeletal elements, the stylopod and zeugopod are genetically under different control than the autopod. The hindlimb phenotype of *Hoxb6Cre*; *Sall4* mutants suggests that *Sall4* alone does not regulate the development of the femur and tibia. Instead, *Sall4* and *Plzf* cooperate in hindlimb buds to regulate *Gli3*, and *Plzf* and *Gli3* regulate development of these elements (Figure 9A). Notably milder skeletal defects and partial downregulation of PLZF in *Hoxb6Cre*; *Sall4* mutant hindlimbs, compared to *TCre*; *Sall4* mutant hindlimbs, also support the model that *Sall4* and *Plzf* cooperate together for hindlimb development.

In the case of femur development, our data support the notion that *Sall4* and *Plzf* also regulate *Hox10* genes. Collectively, this study connected previous studies and uncovered the relationship of genes for the femur development (Wellik and Capecchi 2003; Barna *et al.* 2005). Beside these genes that we connected in this study, a previous study demonstrated that *Irx3/5* dKO hindlimbs also exhibit short femur and loss of tibia (Li *et al.* 2014). A genetic study demonstrated that, in *Drosophila*, *spalt* (*Sall* homolog) regulates *irx* (*Irx* homolog) in the wing imaginal disk (de Celis and Barrio 2000). However, gene expression analysis of *Sall4*; *Plzf* dKO hindlimb bud (this study) and *TCre*; *Sall4* cKO embryos (Akiyama *et al.* 2015) suggests that *Irx3/5* acts in parallel to the *Sall4*-dependent pathway. It has been demonstrated that IRX3 and IRX5 directly regulates *Gli3* through its limb-specific enhancer (Li *et al.* 2014). Therefore, *Gli3* could act as a key regulator of femur development downstream of both the *Sall4* pathway and *Irx3/5* pathway. In the zeugopod, the *Sall4-Plzf-Gli3* system also regulates development of the tibia, the anterior zeugopod element. Given normal development of the tibia in *Hox10*$^{-/-}$ hindlimbs, downstream of the *Sall4-Plzf* system for tibia development is different from femur development. As 45% of *Sall4*; *Plzf* dKO mutants exhibited short fibula, which is a *Shh*-dependent posterior element, the *Sall4-Plzf-Gli3* system may contribute to proliferative expansion of fibula precursors.

Plasticity of digit development programs

It has been considered that d1 develops independent of *Shh*; however, a recent study of *Irx3/5* dKO provided genetic evidence that SHH signaling negatively regulates d1 development (Li *et al.* 2014). Our result is in agreement with this study and suggests that *Sall4*-dependent antagonism against SHH signaling is necessary for d1 development (Figure 9B). It is considered that SHH-dependent patterning along the anterior-posterior axis is completed within 12 hr of the onset of *Shh* expression (Zhu *et al.* 2008). In hindlimb buds, *Shh* expression starts at the 32–33 somite stage (Li *et al.* 2014), by which SALL4 is substantially downregulated in *Hoxb6Cre*; *Sall4* cKO hindlimb bud (Figure 1). These studies are consistent with the proposed time window for *Shh*-dependent digit patterning. Moreover, removing one allele of *Shh* partially rescued d1 development and *Gli1* expression-free anterior domain. These observations support the former report that anterior progenitors are specified early but their fate is not committed until later (Li *et al.* 2014).

Sall4 and Plzf cooperation

Both *Sall4* and *Plzf* are required for maintenance of undifferentiated spermatogonia stem cells in mice (Buaas *et al.* 2004; Costoya *et al.* 2004; Hobbs *et al.* 2012). It has been shown that SALL4 physically interacts with PLZF, and modulates PLZF binding to its targets (Hobbs *et al.* 2012; Lovelace *et al.* 2016). In these studies, SALL4 and PLZF would function in an antagonistic manner or cooperative manner through their physical interaction. Our recent SALL4 chromatin immunoprecipitation followed by sequencing experiments using posterior tissues of E9.5 embryos containing tail buds and presomitic mesoderm resulted in substantially different SALL4-enriched sequences compared to SALL4-bound sequences in mouse embryonic stem cells (Miller *et al.* 2016; Tahara *et al.* 2019). These differences suggested that SALL4 target binding requires cell-type-specific partners. In our genetic experiments, *Sall4*; *Plzf* dKO mice exhibited distinct defects, compared to other combinations of *Sall4*; *Plzf* mutations. This observation suggests that *Sall4* and *Plzf* function in a cooperative manner either by their protein–protein interaction and/or binding to their targets. Further biochemical studies in the future will extend a more detailed understanding of *Sall4-Plzf* function in the limb bud.

SALL4 as a putative target of thalidomide

The hindlimb skeletal defects of *Sall4*; *Plzf* dKO mice are similar to limb defects of people affected by thalidomide exposure [reviewed in Vargesson (2009), Vargesson (2019)]. Deficiencies were more common in forelimbs than hindlimbs, and severely affected individuals exhibited radial dysplasia (loss of the radius and digit 1) or phocomelia (severe shortening of the humerus). In contrast, they retain some structures of the distal autopod. In hindlimbs, the femur is the most commonly affected (Smithells and Newman 1992; Miller and Stromland 2011; Kowalski *et al.* 2015; Vargesson 2019). These proximal anterior skeletal elements (*i.e.*, stylopod, anterior zeugopod, and anterior digits) are either severely defective or missing in *Sall4*; *Plzf* dKO mice. Indeed, *SALL4* was considered as a target of thalidomide (Kohlhase *et al.* 2003; Knobloch and Ruther 2008). Several mechanisms for the thalidomide-induced limb deficiency have been proposed (Vargesson 2009; Vargesson 2019), which include Cereblon (CRBN)-dependent signaling. Thalidomide binds to CRBN (Ito *et al.* 2010), a ubiquitin ligase, which induces CRBN binding to SALL4, leading to degradation of SALL4 protein (Donovan *et al.* 2018; Matyskiela *et al.* 2018). Interestingly, thalidomide action is species specific (Vargesson 2015). The amino acid residues of the SALL4 protein that are required for CRBN-dependent degradation are conserved among thalidomide-sensitive species (*e.g.*, humans), but not in insensitive species (*e.g.*, mice) (Donovan *et al.* 2018; Matyskiela *et al.* 2018). Because of such differences, mouse models did not provide relevant information to study thalidomide-induced teratogenicity. The hindlimb skeletal phenotype obtained by a genetic approach in mice in this study supports the notion that downregulation of *Sall4* function is involved in the thalidomide-induced limb deficiency. Thalidomide can induce global gene expression changes during human embryonic stem cell differentiation (Meganathan *et al.* 2012), and the thalidomide syndrome could involve thousands of downstream genes (Vargesson 2019). Our genetic data suggest that genes and signaling pathways that are regulated by the combined functions of *Sall4* and *Plzf*, such as *Gli3*, *Hox10*, and SHH signaling, are potentially involved in thalidomide-induced limb deficiency.

Acknowledgments

We are grateful to Eric Feil, Jennifer Kim, Cailin McMahon, Aditi Soni, Justin Wang, and Julia Wong for their excellent technical assistance. We are also grateful to Drs. Maria Barna, Mario Capecchi, C-c Hui, Juan Carlos Izpisua Belmonte, and Licia Selleri for providing *in situ* probes; Drs. Mark Lewandoski and Yasushi Nakagawa for mouse lines; Dr. Michael O'Connor for the use of the Zeiss LSM710; and Dr. Naoyuki Wada for critical reading of the manuscript. K.Q.C. and A.A. were partially supported by the University of Minnesota's Undergraduate Research Opportunity Program. This study was supported by a grant from the National Institutes of Health to Y.K. (R01AR064195). The funders had no role in the study design, data collection and analysis, decision to publish, or preparation of the manuscript. The authors declare no competing or financial interests.

Author contributions: K.Q.C., N.T., A.A., H.K., S.K., and Y.K. performed experiments and collected data. R.N. and P.P.P. generated the *Sall4* conditional mouse line and *Plzf* mutant mouse line, respectively. K.Q.C., N.T., A.A., S.K., and Y.K. analyzed data. Y.K. conceived and supervised the study. K.Q.C. and Y.K. wrote the manuscript and all authors edited the manuscript.

Literature Cited

Agarwal, P., J. N. Wylie, J. Galceran, O. Arkhitko, C. Li *et al.*, 2003 Tbx5 is essential for forelimb bud initiation following patterning of the limb field in the mouse embryo. Development 130: 623–633. https://doi.org/10.1242/dev.00191

Agresti, A., 2012 Inference for Two-Way Contingency Tables, pp. 69–112 in *Categorical Data Analysis*. Wiley, Hoboken, NJ.

Ahn, S., and A. L. Joyner, 2004 Dynamic changes in the response of cells to positive hedgehog signaling during mouse limb patterning. Cell 118: 505–516. https://doi.org/10.1016/j.cell.2004.07.023

Akiyama, R., H. Kawakami, J. Wong, I. Oishi, R. Nishinakamura *et al.*, 2015 Sall4-Gli3 system in early limb progenitors is essential for the development of limb skeletal elements. Proc. Natl. Acad. Sci. USA 112: 5075–5080. https://doi.org/10.1073/pnas.1421949112

Anderson, E., S. Peluso, L. A. Lettice, and R. E. Hill, 2012 Human limb abnormalities caused by disruption of hedgehog signaling. Trends Genet. 28: 364–373. https://doi.org/10.1016/j.tig.2012.03.012

Barna, M., N. Hawe, L. Niswander, and P. P. Pandolfi, 2000 Plzf regulates limb and axial skeletal patterning. Nat. Genet. 25: 166–172. https://doi.org/10.1038/76014

Barna, M., P. P. Pandolfi, and L. Niswander, 2005 Gli3 and Plzf cooperate in proximal limb patterning at early stages of limb development. Nature 436: 277–281. https://doi.org/10.1038/nature03801

Buaas, F. W., A. L. Kirsh, M. Sharma, D. J. McLean, J. L. Morris *et al.*, 2004 Plzf is required in adult male germ cells for stem cell self-renewal. Nat. Genet. 36: 647–652. https://doi.org/10.1038/ng1366

Butterfield, N. C., V. Metzis, E. McGlinn, S. J. Bruce, B. J. Wainwright *et al.*, 2009 Patched 1 is a crucial determinant of asymmetry and digit number in the vertebrate limb. Development 136: 3515–3524. https://doi.org/10.1242/dev.037507

Capdevila, J., T. Tsukui, C. Rodriquez Esteban, V. Zappavigna, and J. C. Izpisua Belmonte, 1999 Control of vertebrate limb outgrowth by the proximal factor Meis2 and distal antagonism of BMPs by Gremlin. Mol. Cell 4: 839–849. https://doi.org/10.1016/S1097-2765(00)80393-7

Capellini, T. D., G. Di Giacomo, V. Salsi, A. Brendolan, E. Ferretti *et al.*, 2006 Pbx1/Pbx2 requirement for distal limb patterning is mediated by the hierarchical control of Hox gene spatial distribution and Shh expression. Development 133: 2263–2273. https://doi.org/10.1242/dev.02395

Capellini, T. D., V. Zappavigna, and L. Selleri, 2011 Pbx homeodomain proteins: TALEnted regulators of limb patterning and outgrowth. Dev. Dyn. 240: 1063–1086. https://doi.org/10.1002/dvdy.22605

Chiang, C., Y. Litingtung, E. Lee, K. E. Young, J. L. Corden *et al.*, 1996 Cyclopia and defective axial patterning in mice lacking

Sonic hedgehog gene function. Nature 383: 407–413. https://doi.org/10.1038/383407a0

Chiang, C., Y. Litingtung, M. P. Harris, B. K. Simandl, Y. Li *et al.*, 2001 Manifestation of the limb prepattern: limb development in the absence of sonic hedgehog function. Dev. Biol. 236: 421–435. https://doi.org/10.1006/dbio.2001.0346

Cooper, K. L., J. K. Hu, D. ten Berge, M. Fernandez-Teran, M. A. Ros *et al.*, 2011 Initiation of proximal-distal patterning in the vertebrate limb by signals and growth. Science 332: 1083–1086. https://doi.org/10.1126/science.1199499

Costoya, J. A., R. M. Hobbs, M. Barna, G. Cattoretti, K. Manova *et al.*, 2004 Essential role of Plzf in maintenance of spermatogonial stem cells. Nat. Genet. 36: 653–659. https://doi.org/10.1038/ng1367

Cunningham, T. J., X. Zhao, L. L. Sandell, S. M. Evans, P. A. Trainor *et al.*, 2013 Antagonism between retinoic acid and fibroblast growth factor signaling during limb development. Cell Rep. 3: 1503–1511. https://doi.org/10.1016/j.celrep.2013.03.036

Dassule, H. R., P. Lewis, M. Bei, R. Maas, and A. P. McMahon, 2000 Sonic hedgehog regulates growth and morphogenesis of the tooth. Development 127: 4775–4785.

de Celis, J. F., and R. Barrio, 2000 Function of the spalt/spalt-related gene complex in positioning the veins in the Drosophila wing. Mech. Dev. 91: 31–41. https://doi.org/10.1016/S0925-4773(99)00261-0

de Celis, J. F., and R. Barrio, 2009 Regulation and function of Spalt proteins during animal development. Int. J. Dev. Biol. 53: 1385–1398. https://doi.org/10.1387/ijdb.072408jd

Delgado, I., and M. Torres, 2017 Coordination of limb development by crosstalk among axial patterning pathways. Dev. Biol. 429: 382–386. https://doi.org/10.1016/j.ydbio.2017.03.006

Donovan, K. A., J. An, R. P. Nowak, J. C. Yuan, E. C. Fink *et al.*, 2018 Thalidomide promotes degradation of SALL4, a transcription factor implicated in Duane Radial Ray syndrome. eLife 7: e38430. https://doi.org/10.7554/eLife.38430

Harfe, B. D., P. J. Scherz, S. Nissim, H. Tian, A. P. McMahon *et al.*, 2004 Evidence for an expansion-based temporal Shh gradient in specifying vertebrate digit identities. Cell 118: 517–528. https://doi.org/10.1016/j.cell.2004.07.024

Hobbs, R. M., S. Fagoonee, A. Papa, K. Webster, F. Altruda *et al.*, 2012 Functional antagonism between Sall4 and Plzf defines germline progenitors. Cell Stem Cell 10: 284–298. https://doi.org/10.1016/j.stem.2012.02.004

Hui, C. C., and A. L. Joyner, 1993 A mouse model of greig cephalopolysyndactyly syndrome: the extra-toesJ mutation contains an intragenic deletion of the Gli3 gene. Nat. Genet. 3: 241–246 [corrigenda: Nat. Genet. 19: 404 (1998)]. https://doi.org/10.1038/ng0393-241

Hui, C. C., and S. Angers, 2011 Gli proteins in development and disease. Annu. Rev. Cell Dev. Biol. 27: 513–537. https://doi.org/10.1146/annurev-cellbio-092910-154048

Ito, T., H. Ando, T. Suzuki, T. Ogura, K. Hotta *et al.*, 2010 Identification of a primary target of thalidomide teratogenicity. Science 327: 1345–1350. https://doi.org/10.1126/science.1177319

Itou, J., H. Kawakami, T. Quach, M. Osterwalder, S. M. Evans *et al.*, 2012 Islet1 regulates establishment of the posterior hindlimb field upstream of the Hand2-Shh morphoregulatory gene network in mouse embryos. Development 139: 1620–1629. https://doi.org/10.1242/dev.073056

Jain, D., S. Nemec, M. Luxey, Y. Gauthier, A. Bemmo *et al.*, 2018 Regulatory integration of Hox factor activity with T-box factors in limb development. Development 145: dev159830. https://doi.org/10.1242/dev.159830

Johnson, D. R., 1967 Extra-toes: anew mutant gene causing multiple abnormalities in the mouse. J. Embryol. Exp. Morphol. 17: 543–581.

Knobloch, J., and U. Ruther, 2008 Shedding light on an old mystery: thalidomide suppresses survival pathways to induce limb defects. Cell Cycle 7: 1121–1127. https://doi.org/10.4161/cc.7.9.5793

Kohlhase, J., M. Heinrich, M. Liebers, L. Frohlich Archangelo, W. Reardon *et al.*, 2002 Cloning and expression analysis of SALL4, the murine homologue of the gene mutated in Okihiro syndrome. Cytogenet. Genome Res. 98: 274–277. https://doi.org/10.1159/000071048

Kohlhase, J., L. Schubert, M. Liebers, A. Rauch, K. Becker *et al.*, 2003 Mutations at the SALL4 locus on chromosome 20 result in a range of clinically overlapping phenotypes, including Okihiro syndrome, Holt-Oram syndrome, acro-renal-ocular syndrome, and patients previously reported to represent thalidomide embryopathy. J. Med. Genet. 40: 473–478. https://doi.org/10.1136/jmg.40.7.473

Kowalski, T. W., M. T. Sanseverino, L. Schuler-Faccini, and F. S. Vianna, 2015 Thalidomide embryopathy: follow-up of cases born between 1959 and 2010. Birth Defects Res. A Clin. Mol. Teratol. 103: 794–803. https://doi.org/10.1002/bdra.23376

Kraus, P., D. Fraidenraich, and C. A. Loomis, 2001 Some distal limb structures develop in mice lacking Sonic hedgehog signaling. Mech. Dev. 100: 45–58. https://doi.org/10.1016/S0925-4773(00)00492-5

Lanctot, C., A. Moreau, M. Chamberland, M. L. Tremblay, and J. Drouin, 1999 Hindlimb patterning and mandible development require the Ptx1 gene. Development 126: 1805–1810.

Li, D., R. Sakuma, N. A. Vakili, R. Mo, V. Puviindran *et al.*, 2014 Formation of proximal and anterior limb skeleton requires early function of Irx3 and Irx5 and is negatively regulated by Shh signaling. Dev. Cell 29: 233–240. https://doi.org/10.1016/j.devcel.2014.03.001

Liu, T. M., E. H. Lee, B. Lim, and N. Shyh-Chang, 2016 Concise review: balancing stem cell self-renewal and differentiation with PLZF. Stem Cells 34: 277–287. https://doi.org/10.1002/stem.2270

Logan, M., and C. J. Tabin, 1999 Role of Pitx1 upstream of Tbx4 in specification of hindlimb identity. Science 283: 1736–1739. https://doi.org/10.1126/science.283.5408.1736

Lopez-Rios, J., 2016 The many lives of SHH in limb development and evolution. Semin. Cell Dev. Biol. 49: 116–124. https://doi.org/10.1016/j.semcdb.2015.12.018

Lovelace, D. L., Z. Gao, K. Mutoji, Y. C. Song, J. Ruan *et al.*, 2016 The regulatory repertoire of PLZF and SALL4 in undifferentiated spermatogonia. Development 143: 1893–1906. https://doi.org/10.1242/dev.132761

Lowe, L. A., S. Yamada, and M. R. Kuehn, 2000 HoxB6-Cre transgenic mice express Cre recombinase in extra-embryonic mesoderm, in lateral plate and limb mesoderm and at the midbrain/hindbrain junction. Genesis 26: 118–120. https://doi.org/10.1002/(SICI)1526-968X(200002)26:2<118::AID-GENE5>3.0.CO;2-S

Mariani, F. V., C. P. Ahn, and G. R. Martin, 2008 Genetic evidence that FGFs have an instructive role in limb proximal-distal patterning. Nature 453: 401–405. https://doi.org/10.1038/nature06876

Matyskiela, M. E., S. Couto, X. Zheng, G. Lu, J. Hui *et al.*, 2018 SALL4 mediates teratogenicity as a thalidomide-dependent cereblon substrate. Nat. Chem. Biol. 14: 981–987. https://doi.org/10.1038/s41589-018-0129-x

McDonald, J. H., 2008b Tests for nominal variables, pp. 21–87 in *Handbook of Biological Statistics*. Sparky House Publishing, Baltimore, MA.

McDonald, J. H., 2008a Miscellany, pp. 242–287 in *Handbook of Biological Statistics*. Sparky House Publishing, Baltimore, MA.

Meganathan, K., S. Jagtap, V. Wagh, J. Winkler, J. A. Gaspar *et al.*, 2012 Identification of thalidomide-specific transcriptomics and proteomics signatures during differentiation of human embryonic stem cells. PLoS One 7: e44228. https://doi.org/10.1371/journal.pone.0044228

Mercader, N., E. Leonardo, N. Azpiazu, A. Serrano, G. Morata *et al.*, 1999 Conserved regulation of proximodistal limb axis development by Meis1/Hth. Nature 402: 425–429. https://doi.org/10.1038/46580

Mercader, N., E. Leonardo, M. E. Piedra, A. C. Martinez, M. A. Ros *et al.*, 2000 Opposing RA and FGF signals control proximodistal vertebrate limb development through regulation of Meis genes. Development 127: 3961–3970.

Miller, M. T., and K. K. Stromland, 2011 What can we learn from the thalidomide experience: an ophthalmologic perspective. Curr. Opin. Ophthalmol. 22: 356–364. https://doi.org/10.1097/ICU.0b013e3283499f24

Miller, A., M. Ralser, S. L. Kloet, R. Loos, R. Nishinakamura *et al.*, 2016 Sall4 controls differentiation of pluripotent cells independently of the Nucleosome Remodelling and Deacetylation (NuRD) complex. Development 143: 3074–3084. https://doi.org/10.1242/dev.139113

Naiche, L. A., and V. E. Papaioannou, 2007 Tbx4 is not required for hindlimb identity or post-bud hindlimb outgrowth. Development 134: 93–103. https://doi.org/10.1242/dev.02712

Perantoni, A. O., O. Timofeeva, F. Naillat, C. Richman, S. Pajni-Underwood *et al.*, 2005 Inactivation of FGF8 in early mesoderm reveals an essential role in kidney development. Development 132: 3859–3871. https://doi.org/10.1242/dev.01945

Riddle, R. D., R. L. Johnson, E. Laufer, and C. Tabin, 1993 Sonic hedgehog mediates the polarizing activity of the ZPA. Cell 75: 1401–1416. https://doi.org/10.1016/0092-8674(93)90626-2

Rosello-Diez, A., M. A. Ros, and M. Torres, 2011 Diffusible signals, not autonomous mechanisms, determine the main proximodistal limb subdivision. Science 332: 1086–1088. https://doi.org/10.1126/science.1199489

Sakaki-Yumoto, M., C. Kobayashi, A. Sato, S. Fujimura, Y. Matsumoto *et al.*, 2006 The murine homolog of SALL4, a causative gene in Okihiro syndrome, is essential for embryonic stem cell proliferation, and cooperates with Sall1 in anorectal, heart, brain and kidney development. Development 133: 3005–3013. https://doi.org/10.1242/dev.02457

Schneider, I., and N. H. Shubin, 2013 The origin of the tetrapod limb: from expeditions to enhancers. Trends Genet. 29: 419–426. https://doi.org/10.1016/j.tig.2013.01.012

Sears, K. E., J. A. Maier, M. Rivas-Astroza, R. Poe, S. Zhong *et al.*, 2015 The relationship between gene network structure and expression variation among individuals and species. PLoS Genet. 11: e1005398. https://doi.org/10.1371/journal.pgen.1005398

Smithells, R. W., and C. G. Newman, 1992 Recognition of thalidomide defects. J. Med. Genet. 29: 716–723. https://doi.org/10.1136/jmg.29.10.716

Sweetman, D., and A. Munsterberg, 2006 The vertebrate spalt genes in development and disease. Dev. Biol. 293: 285–293. https://doi.org/10.1016/j.ydbio.2006.02.009

Szeto, D. P., C. Rodriguez-Esteban, A. K. Ryan, S. M. O'Connell, F. Liu *et al.*, 1999 Role of the Bicoid-related homeodomain factor Pitx1 in specifying hindlimb morphogenesis and pituitary development. Genes Dev. 13: 484–494. https://doi.org/10.1101/gad.13.4.484

Tabin, C., and L. Wolpert, 2007 Rethinking the proximodistal axis of the vertebrate limb in the molecular era. Genes Dev. 21: 1433–1442. https://doi.org/10.1101/gad.1547407

Tahara, N., H. Kawakami, T. Zhang, D. Zarkower, and Y. Kawakami, 2018 Temporal changes of Sall4 lineage contribution in developing embryos and the contribution of Sall4-lineages to postnatal germ cells in mice. Sci. Rep. 8: 16410. https://doi.org/10.1038/s41598-018-34745-5

Tahara, N., H. Kawakami, K. Q. Chen, A. Anderson, M. Yamashita Peterson *et al.*, 2019 Sall4 regulates neuromesodermal progenitors and their descendants during body elongation in mouse embryos. Development 146: dev177659. https://doi.org/10.1242/dev.177659

Tao, H., Y. Kawakami, C. C. Hui, and S. Hopyan, 2017 The two domain hypothesis of limb prepattern and its relevance to congenital limb anomalies. Wiley Interdiscip. Rev. Dev. Biol. 6: e270. https://doi.org/10.1002/wdev.270

Tickle, C., 2015 How the embryo makes a limb: determination, polarity and identity. J. Anat. 227: 418–430. https://doi.org/10.1111/joa.12361

Tickle, C., and M. Towers, 2017 Sonic hedgehog signaling in limb development. Front. Cell Dev. Biol. 5: 14. https://doi.org/10.3389/fcell.2017.00014

Vargesson, N., 2009 Thalidomide-induced limb defects: resolving a 50-year-old puzzle. BioEssays 31: 1327–1336. https://doi.org/10.1002/bies.200900103

Vargesson, N., 2015 Thalidomide-induced teratogenesis: history and mechanisms. Birth Defects Res. C Embryo Today 105: 140–156. https://doi.org/10.1002/bdrc.21096

Vargesson, N., 2019 The teratogenic effects of thalidomide on limbs. J. Hand Surg. Eur. Vol. 44: 88–95. https://doi.org/10.1177/1753193418805249

Wellik, D. M., and M. R. Capecchi, 2003 Hox10 and Hox11 genes are required to globally pattern the mammalian skeleton. Science 301: 363–367. https://doi.org/10.1126/science.1085672

Zeller, R., J. Lopez-Rios, and A. Zuniga, 2009 Vertebrate limb bud development: moving towards integrative analysis of organogenesis. Nat. Rev. Genet. 10: 845–858. https://doi.org/10.1038/nrg2681

Zhao, X., I. O. Sirbu, F. A. Mic, N. Molotkova, A. Molotkov *et al.*, 2009 Retinoic acid promotes limb induction through effects on body axis extension but is unnecessary for limb patterning. Curr. Biol. 19: 1050–1057. https://doi.org/10.1016/j.cub.2009.04.059

Zhulyn, O., D. Li, S. Deimling, N. A. Vakili, R. Mo *et al.*, 2014 A switch from low to high Shh activity regulates establishment of limb progenitors and signaling centers. Dev. Cell 29: 241–249. https://doi.org/10.1016/j.devcel.2014.03.002

Zhu, J., E. Nakamura, M. T. Nguyen, X. Bao, H. Akiyama *et al.*, 2008 Uncoupling Sonic hedgehog control of pattern and expansion of the developing limb bud. Dev. Cell 14: 624–632. https://doi.org/10.1016/j.devcel.2008.01.008

Zuniga, A., 2015 Next generation limb development and evolution: old questions, new perspectives. Development 142: 3810–3820. https://doi.org/10.1242/dev.125757

Communicating editor: B. Draper